J. Membrane Biol. 4, 358–394 (1971)

The Mechanism of Cation Permeation in Rabbit Gallbladder

Dilution Potentials and Biionic Potentials

PETER H. BARRY, JARED M. DIAMOND, and ERNEST M. WRIGHT

Department of Physiology, University of California Medical Center,
Los Angeles, California 90024

Received 8 September 1970

Summary. The experimental measurements of passive ion permeation in rabbit gall bladder presented in this paper include: single-salt dilution potentials as a function o concentration gradient; comparison of dilution potentials for different alkali chlorides comparison of biionic potentials for different alkali chlorides; and biionic mixtur potentials as a function of cation concentration gradient. Both dilution potentials an biionic potentials yield the permeability sequence $K^+ > Rb^+ > Na^+ > Li^+ > Cs^+$, a sequence consistent with simple considerations of ion-site interactions and ion hydratio energies. Construction of empirical selectivity isotherms for alkali cation permeatio in epithelia shows that permeability ratios are nearer one in the gallbladder and othe epithelia than in most other biological membranes, indicating a relatively hydrate permeation route. Evaluation of the results of this and the preceding paper suggest the following: that cations permeate gallbladder epithelium via channels with fixe neutral sites; that the rate-controlling membrane is thick enough that microscopi electroneutrality must be obeyed; that virtually all anion conductance is in a shun which develops with time after dissection; that apparent permeability changes wit solution composition are due to the non-ideal activity factor n being less than 1.0; tha effects of pH, Ca^{++}, and ionic strength may involve changes in the anion/cation mobilit ratio owing to changes in wall charges or dipoles; and that the permeation route ma reside in the tight junctions. A similar mechanism may be applicable to cation permeatio in other epithelia.

This paper reports the analysis of alkali chloride dilution potentials an biionic potentials in rabbit gallbladder, to conclude the presentation begu in the previous three papers (Barry & Diamond, 1970 – referred to here after as I; Barry & Diamond, 1971 – referred to hereafter as II; Wright Barry & Diamond, 1971 – referred to hereafter as III) concerning th mechanism of cation permeation in this epithelium. The several types o experimental results are then confronted, and a model permeation mecha nism consistent with the results is suggested. An appendix derives th equations describing a cation exchanger in parallel with a shunt.

Methods

Experimental methods are discussed in II and III.

Errors are quoted as standard errors of the mean.

Regarding mathematical analysis of the results and extraction of relative permeability coefficients, the equations believed to be the most nearly correct and physically realistic ones to use for the gallbladder are those describing a thick fixed-neutral-site membrane in parallel with a free-solution shunt (paper II, model 2). For some preliminary analysis in the Results section before presenting the evidence for the fixed-neutral-site model, we use the Goldman-Hodgkin-Katz equation or so-called "constant-field equation" (Goldman, 1943; Hodgkin & Katz, 1949), because this equation is the one most commonly used by biologists, it is easy to use (i.e., does not require a computer for its solution, unlike the fixed-neutral-site equations), and it turns out to give calculated permeability ratios close to the values extracted from the fixed-neutral-site equations. The fairly good fit to the gallbladder results provided by the Goldman-Hodgkin-Katz equation does not necessarily imply a constant field in the membrane, since this equation can be valid for a membrane solely permeable to ions of one sign without the necessity of the field being constant (Sandblom & Eisenman, 1967). For a system consisting of two cations M^+ and N^+ and one anion Cl^-, the Goldman-Hodgkin-Katz equation assumes the form

$$E''-E'=\frac{-RT}{F}\ln\frac{P_M[M^+]''+P_N[N^+]''+P_{Cl}[Cl^-]'}{P_M[M^+]'+P_N[N^+]'+P_{Cl}[Cl^-]''} \tag{1}$$

where superscripts $'$ and $''$ refer to the mucosal and serosal bathing solutions, respectively; E is the electrical potential in mV; the factor RT/F equals 25.5 mV at 23 °C; P's are relative permeability coefficients; and quantities in brackets are activities. A third set of equations, those describing a macroscopic cation exchanger in parallel with a free-solution shunt (derived in the appendix), was used only to analyze dilution potentials as a function of gradient (Fig. 2), in order to illustrate that this model gives a poor fit to the results and can be excluded.

Calculations were carried out on an IBM 360 computer, using APL language. All calculations used activities rather than concentrations, based on single-ion activity coefficients taken from tabulated mean values (Robinson & Stokes, 1965) using the so-called Guggenheim assumption (*see* paper I, p. 104). Throughout this paper, brackets will be used to represent activities, parentheses for concentrations.

Results

Dilution Potentials as a Function of Gradient

The salt chosen for measurements of dilution potentials [i.e., potential differences (p.d.) resulting from a concentration gradient of a single salt] as a function of concentration gradient was CsCl. We made this choice partly in order to minimize junction potential corrections; and partly because such measurements would be an insensitive test of the permeation mechanism if the cation/anion permeability ratio were very high (i.e., if the p.d.'s predicted by any model tended to Nernst values), and Cs^+ has

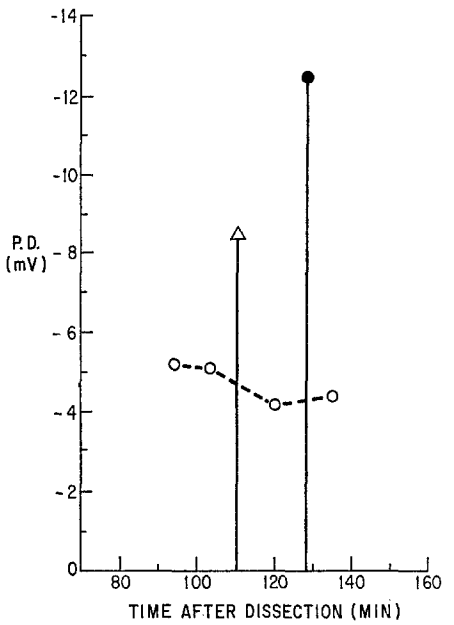

Fig. 1. CsCl dilution potentials as a function of concentration gradient. The serosa solution was 150 mM CsCl throughout the experiment, and p.d.'s were measured when the mucosal solution was 75 mM (○), 37.5 mM (△), or 18.75 mM (●) CsCl to create 2:1, 4:1, and 8:1 gradients. The vertical lines indicate times when the p.d. resulting from 4:1 or 8:1 gradient was compared with the p.d. from a 2:1 gradient

the advantage that its permeability is nearer P_{Cl} than is the permeability of any other alkali cation. As illustrated in Fig. 1, the experimental procedure consisted of taking 150 mM CsCl as both the mucosal and serosal solutions, then measuring 2:1, 4:1, and 8:1 dilution potentials by changing the mucosal solution to 75, 37.5, or 18.75 mM CsCl, all solutions being kept isoosmotic with 150 mM CsCl by incorporation of mannitol. Measurement at 37.5 or at 18.75 mM were bracketed by measurements at 75 mM.

Fig. 2 illustrates the results of three such experiments. To compensate for variation in p.d.'s with time during an experiment, the parameters were normalized by the procedure described below[1] to correspond to the average

1 Normalization procedures based on different model equations all yielded virtually the same results. The particular procedure used in constructing Fig. 2 was as follows. The $Cl^-:Cs^+$ permeability ratio α was extracted from the p.d. for each gradient in each experiment by means of the thick fixed-neutral-site model plus shunt with $n=0$. [paper II, Eq. (53), $u_3=0$, $\alpha \equiv \lambda_s A_n v_3/u_1(K_1K_3)^{1/2n}$]. First, $\alpha_{av}(150:75)$ was calculated for a 150:75 mM gradient using the average p.d. of -5.0 mV for this gradient in the series of experiments. At a time in an experiment selected for comparison of p.d. (e.g., vertical lines, Fig. 1), $\alpha(150:75)$ and either $\alpha(150:37.5)$ or $\alpha(150:18.75)$ were calculated from the interpolated values of the p.d.'s. $\alpha(150:37.5)$ or $\alpha(150:18.75)$ was

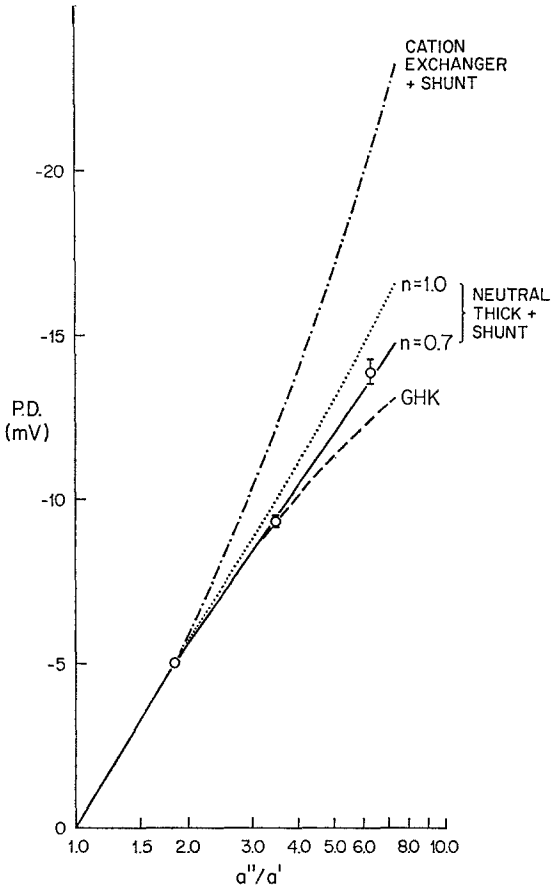

Fig. 2. Comparison of experimental dilution potentials with predictions of four model equations. The experimental points (⊖) are the dilution potentials resulting from CsCl gradients, measured as in Fig. 1 and normalized as described in footnote 1. The abscissa is the CsCl activity ratio (activity in serosal solution divided by activity in mucosal solution), plotted on a logarithmic scale. Theoretical curves fitted to pass through the point at an activity ratio of 1.84 (150:75 mM concentration gradient) have been calculated from the model of a cation exchanger plus shunt [Appendix, Eq. (8), —·—·], from the model of a thick fixed-neutral-site membrane plus shunt with the non-ideal activity factor n taken as 1 [paper II, Eq. (53), ·····], from the same model with n taken as 0.7 (——), and from the Goldman-Hodgkin-Katz equation [Eq. (1), — — —]. The fit is good to the first three models but poor to the cation exchanger-plus-shunt model

then multiplied by the ratio $\alpha(150:75)/\alpha_{av}(150:75)$, which was generally close to 1, to yield normalized α's for these gradients. Finally, these normalized α's were inserted back into Eq. (53) of paper II to yield the normalized p.d.'s displayed in Fig. 2. The p.d.'s normalized according to three other model equations [Goldman-Hodgkin-Katz equation (Eq. 1), thick fixed-neutral-site model with $n=1$ and without shunt (paper II, Eq. 42), cation-exchanger-plus-shunt equation (Appendix, Eq. 8)] differ on the average by only 0.1 mV from these normalized p.d.'s obtained from the thick fixed-neutral-site model plus shunt with $n=0.7$.

150:75 mM dilution potential of −5.0 mV, and the average normalized p.d.'s for each gradient are plotted as the experimental points of Fig. 2. Fig. 2 also shows theoretical curves derived from four different model equations (cation-exchanger-plus shunt (−·−·−·), thick fixed-neutral-site membrane plus shunt with the so-called non-ideal activity factor n taken as 1 (·····), the same model with n taken as 0.7 (——), and the Goldman-Hodgkin-Katz equation (− − −), each fitted to pass through the experimental p.d. for a 150:75 mM gradient (activity ratio of 1.84).

It is apparent from Fig. 2 that the points are fitted well or fairly well by the latter three models but are poorly fitted by the cation exchanger plus-shunt equation. The poor fit to the cation exchanger-plus-shunt model makes it unlikely, as does much other evidence also (pp. 376–377; paper III pp. 351–352), that this model is the correct interpretation of ion permeation in the gallbladder. The curve for a thick fixed-neutral-site membrane plus shunt with $n=1$ passes slightly above the experimental points, but a good fit can be obtained with this model by choosing $n=0.7$. (Without other evidence, one might hesitate on this basis alone to conclude that n is less than 1, but this conclusion will be confirmed more clearly by an analysis of biionic potentials—*see* pp. 383–385, where the meaning of n is discussed.) We have also calculated, but not depicted in Fig. 2, the curves for a thin fixed-neutral-site membrane with or without shunt [paper II, Eqs. (110) or (99)]; as with the corresponding thick-membrane curves, these curves are slightly high with n taken as 1 but yield a close fit with lower values of n. Finally, the Goldman-Hodgkin-Katz equation gives a good fit at low gradients but becomes increasingly discrepant at larger gradients.

An alternative way to test good fit with various equations is to compare the permeability ratios P_{Cl}/P_{Cs} calculated from the experimental p.d.'s for a 2:1, 4:1, and 8:1 gradient. The permeability ratio is virtually independent of gradient when calculated from the thick fixed-neutral-site membrane with $n=0.7$, slightly dependent on the gradient when calculated from this equation with $n=1$ or from the Goldman-Hodgkin-Katz equation, and markedly dependent on the gradient when calculated from the cation exchanger-plus-shunt equation. This illustrates the general point that an apparent change in permeability ratios of a biological membrane with change in solution composition may actually be an artifact of using the wrong model equation to extract permeability ratios.

Dilution Potential Sequences and Biionic Potential Sequences

Cation permeability sequences were obtained from two different types of experiments measuring p.d.'s as a function of concentration gradients

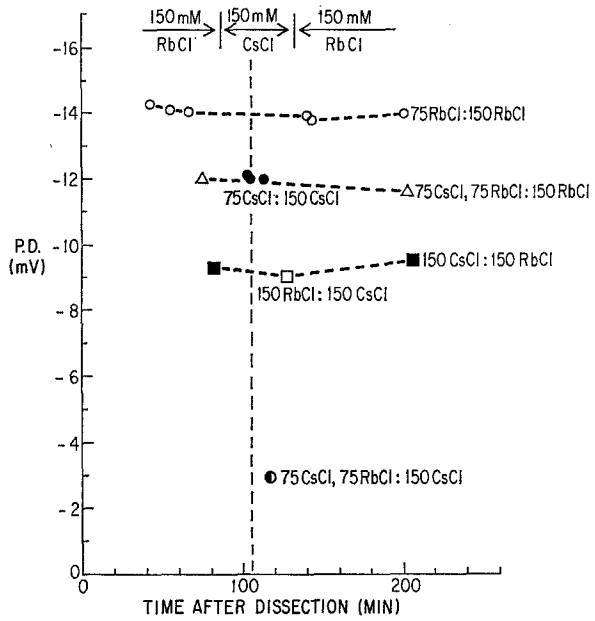

Fig. 3. Dilution potentials and biionic potentials in CsCl and RbCl. P.d.'s were measured when the gallbladder separated the following pairs of solutions, listing the mucosal solution first and the serosal solution second in each case: dilution potentials, 75 mM RbCl vs. 150 mM RbCl ○, 75 mM CsCl vs. 150 mM CsCl ●; biionic potentials, 150 mM RbCl vs. 150 mM CsCl □, 150 mM CsCl vs. 150 mM RbCl ■, 75 mM RbCl–75 mM CsCl vs. 150 mM RbCl △, 75 mM RbCl–75 mM CsCl vs. 150 mM CsCl ◐. The ordinate gives the potential of the serosal solution with respect to that of the mucosal solution, except that the potential of point □ has been reversed in sign to facilitate comparisons. The composition of the serosal solution is indicated by the arrows at the top of the figure. The vertical line indicates the time at which p.d.'s corresponding to different gradients were compared

(1) comparison of 2:1 dilution potentials (p.d.'s resulting from 150 mM M^+Cl^- vs. 75 mM M^+Cl^-) for different alkali chlorides; and (2) comparison of biionic potentials (p.d.'s resulting from 150 mM M^+Cl^- vs. 150 mM N^+Cl^-). It proved most convenient to compare either two or three salts in the same gallbladder. A typical experiment is depicted in Fig. 3, which illustrates the "bracketed" experimental designs utilizing repeated measurements and the interpolation procedure used for comparing several types of dilution potentials and biionic potentials at the same time. In all, Cs^+ and Rb^+ were compared in six experiments, K^+ and Rb^+ in two, Li^+ and Cs^+ in five, Na^+ and K^+ in 16, Li^+ and Na^+ in four, and Cs^+ and Na^+ in four.

Table 1 summarizes the results of all individual experiments. Column 3 gives the dilution potential for one salt, column 4 the dilution potential

Table 1. *P.d.'s and cation permeability ratios in individual experiments* [a]

Cations compared	Exp. no.	p.d.'s (mV)			Permeability ratios	
		Dilution potentials [b]		Biionic potentials [c]	From dilution potentials [d]	From biionic potentials [e]
		E_{RbCl}	E_{CsCl}	$E_{RbCl:CsCl}$	P_{Cs}/P_{Rb}	P_{Cs}/P_{Rb}
Rb:Cs	15	−14.0	−12.0	9.2	0.43	0.61
	17	−12.2	− 9.8	9.3	0.50	0.55
	19	−10.0	− 5.4	7.8	0.31	0.53
	20	−11.4	− 8.8	5.8	0.50	0.69
	21	−11.5	− 6.3	8.8	0.25	0.55
	26	−10.7	− 7.6	9.5	0.45	0.48
					$\overline{0.41 \pm 0.04}$	avg. $\overline{0.57 \pm 0.03}$
		E_{KCl}	E_{RbCl}	$E_{KCl:RbCl}$	P_{Rb}/P_{K}	P_{Rb}/P_{K}
K:Rb	42	−10.7	− 8.9	4.2	0.62	0.73
	43	−11.0	−10.5	3.0	0.88	0.81
					$\overline{0.75 \pm 0.13}$	avg. $\overline{0.77 \pm 0.04}$
		E_{CsCl}	E_{LiCl}	$E_{CsCl:LiCl}$	P_{Li}/P_{Cs}	P_{Li}/P_{Cs}
Cs:Li	27	− 6.0	− 4.7	+0.5	1.07	1.36
	28	− 5.3	− 6.7	−0.9	1.87	1.65
	29	− 6.4	− 5.5	+4.4	1.11	0.93
	31	− 6.2	− 4.5	+3.9	0.98	0.99
	61	− 8.3	− 8.5	−0.1	1.18	1.20
					$\overline{1.24 \pm 0.16}$	avg. $\overline{1.23 \pm 0.13}$
		E_{KCl}	E_{NaCl}	$E_{KCl:NaCl}$	P_{Na}/P_{K}	P_{Na}/P_{K}
K:Na	48a	− 7.6	− 5.6	14.8	0.76	0.18
	48b	−11.2	− 5.4	18.8	0.29	0.24
	49a	−11.8	− 6.9	20.3	0.32	0.23
	49b	− 9.3	− 4.8	19.5	0.43	0.12
	49c	−11.6	− 6.2	20.2	0.30	0.23
	50a	−12.5	− 8.0	16.3	0.33	0.36
	50b	−13.1	− 8.1	20.1	0.26	0.29
	50c	−12.9	− 8.2	22.3	0.29	0.23
	50d	−12.5	− 8.2	15.2	0.34	0.39
	51a	−13.4	−10.7	19.8	0.41	0.30
	51b	−13.7	−10.5	15.0	0.33	0.43
	51c	−12.8	−10.0	14.7	0.44	0.41
	51d	−12.8	− 9.8	23.8	0.42	0.20
	51e	−11.3	− 9.8	13.9	0.70	0.39
	51f	−11.3	− 9.8	21.7	0.70	0.18
	53	−12.3	− 6.7	17.9	0.26	0.31
					$\overline{0.41 \pm 0.04}$	avg. $\overline{0.28 \pm 0.0}$

Table 1 (continued)

Cations compared	Exp. no.	p.d.'s (mV)			Permeability ratios	
		Dilution potentials [b]		Biionic potentials [c]	From dilution potentials [d]	From biionic potentials [e]
		E_{NaCl}	E_{LiCl}	$E_{NaCl:LiCl}$	P_{Li}/P_{Na}	P_{Li}/P_{Na}
Na:Li	54	− 5.7	− 2.6	2.2	0.62	0.90
	56	− 9.4	− 7.3	2.1	0.67	0.89
	57	− 7.4	− 4.2	2.1	0.59	0.90
	58	− 7.5	− 5.7	2.1	0.76	0.90
					$\overline{0.66} \pm 0.04$	avg. $\overline{0.90} \pm 0.00$
		E_{NaCl}	E_{CsCl}	$E_{NaCl:CsCl}$	P_{Cs}/P_{Na}	P_{Cs}/P_{Na}
Na:Cs	58a	− 8.8	− 7.3	2.6	0.63	0.70
	58b	− 7.5	− 7.2	2.5	0.81	0.64
	59	− 4.9	− 5.0	2.6	0.75	0.41
	60	− 8.8	− 5.6	2.5	0.40	0.71
					$\overline{0.65} \pm 0.09$	avg. $\overline{0.62} \pm 0.07$

[a] Results are given for all individual experiments in which permeabilities of two alkali cations were compared by measuring dilution potentials and biionic potentials. Note that there is fair or good agreement between permeability ratios calculated from dilution potentials and from biionic potentials.

[b] For a 150:75 mM gradient of each alkali cation chloride.

[c] Between 150 mM solutions of the two alkali cation chlorides, listing the one in the mucosal solution first and the one in the serosal solution second (since the p.d. is given as the potential of the serosal solution with respect to that of the mucosal solution, a positive sign means that the first cation is more permeant than the second).

[d] The permeability ratio extracted from the two dilution potentials by the equation for a thick membrane with fixed neutral sites and shunt, taking the non-ideal activity factor n as 0.8 [$u_1(K_1K_3)^{1/2n}/\lambda_s A_n v_3$ was calculated for each salt from paper II, Eq. (53), setting $u_3=0$, and the ratio was taken of the values for the two salts].

[e] The permeability ratio extracted from the biionic potential by the equation for a thin membrane with fixed neutral sites and shunt, taking n as 0.8 [$u_2K_2^{1/n}/u_1K_1^{1/n}$ in paper II, Eq. (113), setting $u_3=0$].

for a second salt, and column 5 the biionic potential between the two salts. Columns 6 and 7, which give cation permeability ratios extracted from these p.d.'s by means of the equations describing a membrane with fixed neutral sites, will be discussed later.

For a preliminary analysis of these experimental results, we extracted permeability ratios from the measured p.d.'s by means of the simple and commonly used Goldman-Hodgkin-Katz equation [(Eq. (1)]. From the

Table 2. *Cation permeability ratios calculated from the Goldman-Hodgkin-Katz equation* [*Eq.* (1)][a]

Cation	Permeability relative to Na^+		No. of measurements	No. of gallbladders
	From dilution potentials	From biionic potentials		
K^+	2.3 ±0.2	2.4 ±0.1	16	5
Rb^+	1.8 ±0.3	1.7 ±0.4	6	5
Na^+	1.0	1.0		
Cs^+	0.86±0.10	0.90±0.01	8	7
Li^+	0.73±0.10	0.84±0.05	4	3

[a] Cation permeability ratios (P_{M^+}/P_{N^+}) were calculated from pairs of dilution potentials (as the ratio of P_M/P_{Cl} to P_N/P_{Cl}) and from biionic potentials, for all the individual experiments listed in Table 1, and the results were averaged. P_K/P_{Na} and P_{Cs}/P_{Na} were obtained from experiments in which these pairs of ions were compared directly. P_{Li}/P_{Na} was taken not only from direct comparisons of Li^+ and Na^+, but also by calculating P_{Li}/P_{Cs} from Li^+–Cs^+ comparisons and multiplying by the average P_{Cs}/P_{Na}. P_{Rb}/P_{Na} was not obtained from direct Rb^+–Na^+ comparisons, but instead by comparing Rb^+–K^+ to obtain P_{Rb}/P_K and multiplying by the average P_K/P_{Na}, and by comparing Rb^+–Cs^+ to obtain P_{Rb}/P_{Cs} and multiplying by the average P_{Cs}/P_{Na}.

summary of the average values of these ratios in Table 2, two features may be noted at this point. The first is that the ratios derived from dilution potentials agree well with the ratios derived from biionic potentials, not only in sequence but also in absolute values. As discussed on pp. 376–377 this is contrary to the expected behavior of an ion-exchange membrane Secondly, the apparent permeability sequence is $K^+ > Rb^+ > Na^+ > Cs^+ > Li^+$. The only respect in which any gallbladder studied deviated from this sequence involved the relative positions of Li^+ and Cs^+. LiCl dilution potentials frequently exceeded CsCl dilution potentials in freshly dissected gallbladders but declined more rapidly with time, so that values of P_{Cs} greater than P_{Li} were usually obtained by the time in the experiment when quantitative comparison of the dilution potentials was made. Similarly the sign of biionic potentials frequently indicated $P_{Li} > P_{Cs}$ in freshly dissected gallbladders but gradually reversed in sign with passage of time This suggests that $P_{Li} > P_{Cs}$ in native gallbladder membrane and that after dissection a shunt pathway gradually develops in which ions move with free-solution mobility ratios ($u_{Cs} > u_{Li}$). This interpretation will be confirmed by further experimental evidence to be presented on pp. 368–371. On

pp. 381–389, we discuss how to correct measured permeability coefficients for the effect of the shunt, and we show that in native gallbladder membrane both dilution potentials and biionic potentials yield the sequence $K^+ > Rb^+ > Na^+ > Li^+ > Cs^+$.

Biionic Mixture Potentials as a Function of Cation Gradients

In five experiments involving the Rb^+–Cs^+ cation pair and in one experiment involving the Na^+–K^+ pair, biionic potentials were determined with mixed salt solutions (e.g., 30 mM RbCl + 120 mM CsCl vs. 150 mM CsCl, or 75 mM RbCl + 75 mM CsCl vs. 150 mM RbCl). Fig. 3 illustrates the experimental procedure. As illustrated in Fig. 4, the trend in all six gallbladders was that the apparent relative permeability of each cation, calculated from the Goldman-Hodgkin-Katz equation [Eq. (1)], increased as its contribution to the mixture proportions increased – e.g., the calculated ratio P_{Cs}/P_{Rb} increased as the concentration ratio $(Cs^+)/[(Rb^+)+(Cs^+)]$ increased. Similar apparent shifts in relative permeability ratios with solution composition have been observed in cation-selective glass electrodes and aluminosilicate ion exchangers (Eisenman, 1962). Their interpretation in terms of the so-called non-ideal activity factor n and site interactions will be discussed on pp. 383–385.

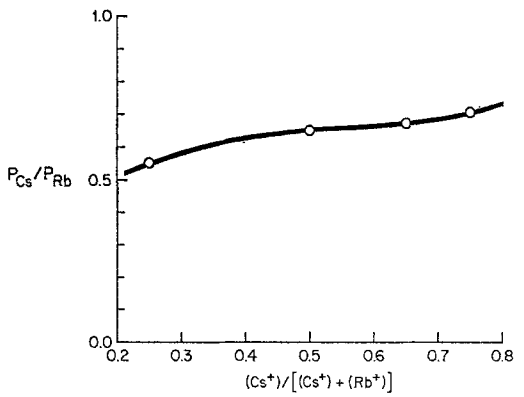

Fig. 4. Cation permeability ratio as a function of mixture composition. The ratio P_{Cs}/P_{Rb} (ordinate) was calculated from biionic potentials in mixed solutions of CsCl and RbCl by means of the Goldman-Hodgkin-Katz equation [Eq. (1)], and is plotted as a function of the average fractional Cs^+ concentration [i.e., $(Cs^+)/[(Cs^+)+(Rb^+)]$] in the two bathing solutions as the abscissa. The curve would be a horizontal straight line if the gallbladder had constant Goldman-Hodgkin-Katz permeability coefficients, but this is evidently not the case. Instead, the more (Cs^+) is present, the more permeant Cs^+ becomes, and the more (Rb^+) is present, the more permeant Rb^+ becomes

Time Dependence of Permeability Sequences

As already mentioned, the permeability properties of *in vitro* gallbladders are not independent of time but undergo slow changes after dissection, mainly during the first 1 to 1½ hr after dissection. Dilution potentials for all alkali halide salts decrease with time, implying that the cation/anion permeability ratios are decreasing. The magnitudes of most biionic potentials also tend to decrease.

These changes were investigated in detail in two experiments; the results of one are illustrated in Fig. 5. In these experiments, the serosal solution was kept constant at 150 mM NaCl, while the mucosal solution was repeatedly changed in succession to 150 mM solutions of the other alkali chlorides in order to record biionic potentials. In addition, the mucosal solution was periodically changed to 75 mM NaCl in order to record the 2:1 NaCl dilution potential. These p.d.'s were followed for 21 hr after dissection and measured again after part of the epithelium had been scraped off. As illustrated in Fig. 5, the 2:1 NaCl dilution potential decreased from an

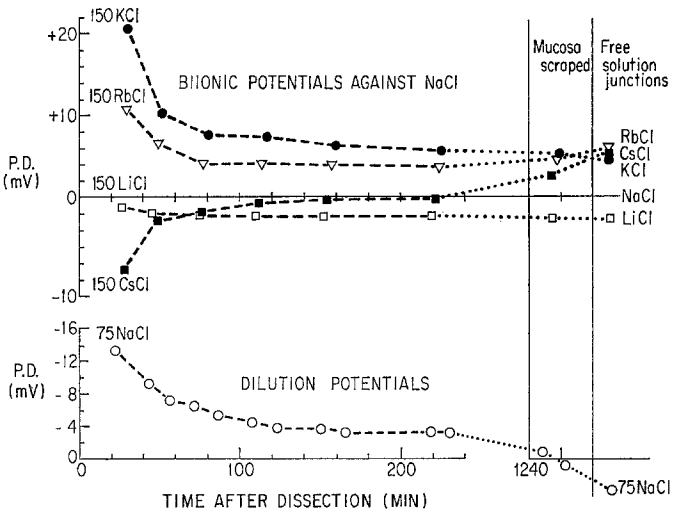

Fig. 5. Diffusion potentials across the gallbladder (ordinate) as a function of time after dissection (abscissa). Throughout the experiment, the serosal bathing solution remained 150 mM NaCl. The mucosal solution was periodically changed to 150 mM solutions of the other alkali chlorides to measure biionic potentials (above), or else to 75 mM NaCl to measure the 2:1 NaCl dilution potential (below). A positive biionic potential means that the indicated cation is more permeant than Na^+; a negative potential means the reverse. After 21 hr, part of the epithelial cell layer was scraped off, and p.d.'s were again measured. The values of the free-solution junction potentials are given on the extreme right for comparison. Note that p.d.'s across the gallbladder gradually decay with time in the direction of the free-solution junction potentials, indicating the development of a free-solution shunt in parallel with native epithelium in the gallbladder

Table 3. *Apparent cation permeability ratios as a function of time* [a]

Cation	P [b]		Relative free-solution mobility
	30 min	120 min	
K^+	2.5 ±0.1	1.7 ±0.1	1.47
Rb^+	1.7 ±0.1	1.4 ±0.1	1.55
Na^+	1.0	1.0	1.0
Li^+	0.90±0.02	0.86±0.01	0.77
Cs^+	0.77±0.07	0.96±0.01	1.54

[a] Apparent cation permeability coefficients relative to Na^+ were measured from biionic potentials at various times after dissection in experiments on two gallbladders, the results of one of which are illustrated in Fig. 5.

[b] Calculated by the Goldman-Hodgkin-Katz equation [Eq. (1)] from values of biionic potentials 30 and 120 min after dissection.

initial value of 13.2 mV. The cation permeability sequence may be deduced from the biionic potentials, the most permeant cation yielding the largest positive p.d. and the least permeant cation the largest negative p.d. Fig. 5 shows that the sequence in freshly dissected gallbladders is $K^+ > Rb^+ > Na^+ > Li^+ > Cs^+$ [sequence VIa in Eisenman's (1961) notation: *see* pp. 371–375 for further discussion of cation selectivity sequences] and changes after a short time to $K^+ > Rb^+ > Na^+ > Cs^+ > Li^+$ (Eisenman's sequence V) owing to an inversion in the Li^+–Cs^+ permeability ratio. Evidence for the same inversion with time was also obtained in dilution potential experiments (p. 366). In addition, the ratio P_{Cs}/P_{Na} gradually approaches 1.0 and finally inverts when part of the epithelium has been scraped off. The average relative permeabilities calculated by means of the Goldman-Hodgkin-Katz equation from p.d.'s measured at 30 and 120 min after dissection in these two gallbladders are given in Table 3.

Both the decline in dilution potentials and the changes in the biionic sequences illustrated in Fig. 5 and Table 3 may be summarized by saying that gallbladder permeability sequences and ratios tend to approach those of the free-solution mobilities with time after the dissection. It will be recalled that conductance also tends to increase for the first 1 to 1½ hr before reaching a steady-state level (paper III, Fig. 3). In order to check the interpretation that a free-shunt solution gradually develops, conductance and NaCl dilution potentials were measured as a function of time after dissection in the same gallbladder (Fig. 6). From the initial value of conductance and of the NaCl dilution potential, subsequent values of the dilution potential were calculated on the basis of each of three hypotheses

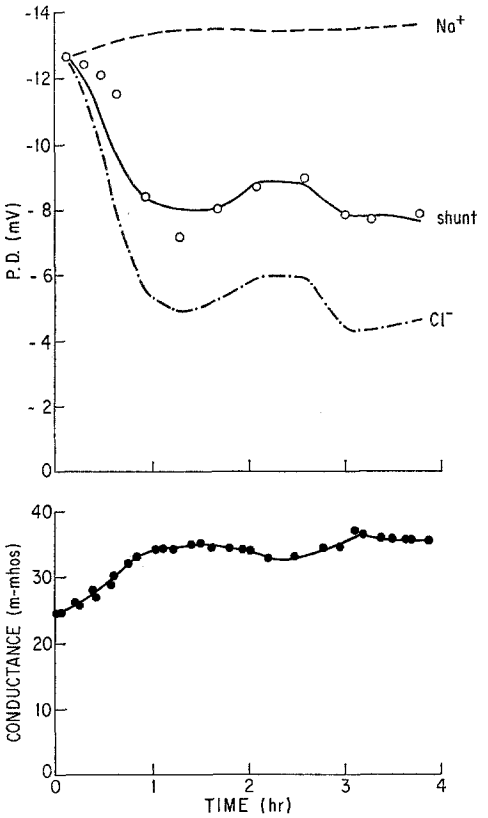

Fig. 6. Comparison of 2:1 NaCl dilution potentials (○) and of conductance in symmetrical 150 mM NaCl solutions (●), measured as a function of time after mounting in the conductance chamber (abscissa). The ratio P_{Cl}/P_{Na} was calculated from the earliest p.d. measurement (12.6 mV at 0.12 hr) by means of the Goldman-Hodgkin-Katz equation to be 0.11. The total measured membrane conductance at 0.12 hr, 25.5 mmhos, must therefore be assigned to partial conductances G_{Cl} and G_{Na} in the same ratio—i.e., $G_{Cl}=\left(\frac{0.11}{1.00+0.11}\right)(25.5)=2.5$ mmhos, $G_{Na}=\left(\frac{1.00}{1.00+0.11}\right)(25.5)=23$ mmhos. The subsequent course of the p.d. with time was then calculated from the subsequent increase in conductance ΔG above 25.5 mmhos, according to three different assumptions. (1) The increase in conductance represents solely an increase in Cl^- conductance, so that P_{Cl}/P_{Na} at any time should equal $(2.5+\Delta G)/23$. These calculated values of P_{Cl}/P_{Na} were inserted into the Goldman-Hodgkin-Katz equation to yield the predicted p.d. curve —·—·—. (2) The increase in conductance represents a free-solution shunt (with transport numbers $t_{Cl}=0.63$, $t_{Na}=0.37$), so that P_{Cl}/P_{Na} at any time should equal $(2.5+0.63\,\Delta G)/(23+0.37\,\Delta G)$, yielding the predicted p.d. curve ——. (3) The increase in conductance represents solely an increase in Na^+ conductance, so that P_{Cl}/P_{Na} at any time should equal $(2.5)/(23+\Delta G)$ yielding the predicted p.d. curve — — — —. Note that the experimental p.d.'s fit the second assumption

concerning the origin of the increase of conductance with time: (1) that it represents solely an increase in Na^+ conductance; (2) that it represents solely an increase in Cl^- conductance; and (3) that it represents the development of a free-solution shunt, i.e. an increase in both the Cl^- and Na^+ conductances in the same proportions as their free-solution mobilities. It appears clear from Fig. 6 that the free-solution shunt gives the closest fit.

Discussion

This discussion section will consider five topics: cation selectivity sequences, anion permeation, the cation permeation mechanism (analyzed qualitatively and in "black-box" terms), mathematical analyses of permeation, and possible structural bases for cation permeation in gallbladder epithelium.

Cation Selectivity Sequences

Perhaps the simplest and most obvious fact about alkali cation permeation in rabbit gallbladder epithelium is that the gallbladder permeability sequence ($K^+ > Rb^+ > Na^+ > Li^+ > Cs^+$: *see* pp. 366, 369 and 388) is not the same as the free-solution mobility sequence or ionic size sequence ($Cs^+ \geqq Rb^+ \geqq K^+ > Na^+ > Li^+$). Similar specific sequences of ion effects, differing both from the sequence of ionic sizes and from the sequence of hydration energies ($Li^+ > Na^+ > K^+ > Rb^+ > Cs^+$), occur in numerous biological systems and in numerous nonliving systems such as glass electrodes and mineral ion exchangers. Although the five alkali cations can be permuted in $5! = 120$ different ways, the great majority of ion potency sequences in nature belong to a pattern composed of only 11 of these permutations plus a few simple variants (Eisenman, 1961, 1962, 1965; Diamond & Wright, 1969). Eisenman showed that these observed sequences can be correctly predicted by comparing the cations' hydration energies with their Coulomb interaction energies with membrane-negative sites of different strengths: very strong membrane sites, such that ion-site attraction energies greatly exceed hydration energies, yield the inverse sequence of ionic sizes $Li^+ > Na^+ > K^+ > Rb^+ > Cs^+$, since the smallest ion is the one most strongly attracted; very weak sites, such that ion-site attraction energies are much less than hydration energies, yield the inverse sequence of hydration energies $Cs^+ > Rb^+ > K^+ > Na^+ > Li^+$, since the most weakly hydrated ion is the one most easily torn out of water; and sites of intermediate strength yield one of nine intermediate sequences. The implication is that biological membranes with different permeability sequences differ in their effective

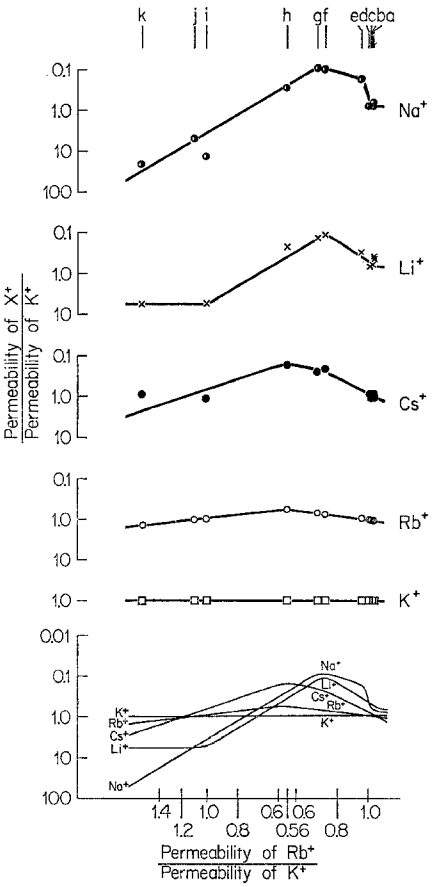

Fig. 7. Selectivity isotherms for the alkali cations in epithelia. The isotherm for each cation together with the experimental points on which it is based is plotted separately above, while all five isotherms are replotted together below without the experimental points. Each set of five experimental points arranged vertically above each other represents relative permeability coefficients extracted from transepithelial potential measurements in one epithelium identified by a letter above: *a* frog gallbladder; *b* frog intestine; *c* rabbit intestine; *d* frog choroid plexus; *e* serosal surface of toad urinary bladder; *f* inside surface of bullfrog skin; *g* inside surface of leopard frog skin; *h* rabbit gallbladder; *i* outside surface of leopard frog skin; *j* mucosal surface of toad urinary bladder; *k* outside surface of bullfrog skin. (Points a through *d* are derived from unpublished measurements by E. M. Wright; *e* and *j* from Leb, Hoshiko & Lindley, 1965; *f*, *g*, *i*, and *k* from Lindley & Hoshiko, 1964; and *h* from the present study.) Permeabilities relative to $P_K = 1$ are plotted logarithmically on the ordinate, and are arranged according to the relative Rb^+ permeability plotted logarithmically on the abscissa. (For instance, permeability coefficients in rabbit gallbladder in the last column of Table 4b of this paper, re-expressed relative to K^+, are: $K^+ = 1.0$, $Rb^+ = 0.56$, $Na^+ = 0.28$, $Li^+ = 0.23$, $Cs^+ = 0.17$. These points have therefore been arranged on an imaginary vertical line intersecting the horizontal axis at 0.56. Since the ordinate gives permeability relative to P_K as a function of P_{Rb}/P_K on the abscissa, the K^+ value automatically falls on a horizontal line intersecting the ordinate at 1.0, and the Rb^+ value automatically falls on

site strengths, and that the electric fields of the biological sites fall off more slowly with distance than does the field of a water molecule (*see* Diamond & Wright, 1969, p. 606, for further discussion).

The gallbladder permeability sequence $K^+ > Rb^+ > Na^+ > Li^+ > Cs^+$, although not one of the 11 permutations predicted by the Coulomb model, is a common variant described as sequence VIa in Eisenman's (1965) terminology, implies sites of intermediate field strength, and differs from sequence V of the Coulomb model ($K^+ > Rb^+ > Na^+ > Cs^+ > Li^+$) only in the inverted positions of Li^+ and Cs^+. Other natural processes exhibiting sequence VIa include cation permeation in glass electrodes composed of 28.3% Na_2O–9.7% Al_2O_3–62% SiO_2 (Eisenman, 1962) and cation-stimulated fermentation by yeast (Rothstein & Demis, 1953). The occurrence of this type of variant, in which Li^+ is more potent than predicted from Coulomb (monopole-monopole) interactions alone, is to be expected if one considers the simplest non-Coulomb forces, namely, ion:induced-dipole forces. If the membrane sites are appreciably more polarizable than are water molecules, then the smallest cation, Li^+, will gain additional energy in its interactions with the site, since it can approach most closely to the site and is the most effective at polarizing. Further examples and discussion of these non-Coulomb sequences and polarization effects are given by Bungenberg de Jong (1949) and by Diamond and Wright (1969).

Alkali cation selectivity in the gallbladder differs from that in most biological systems previously studied in one respect, namely, the low magnitude of selectivity. K^+, the most permeant cation, is only about five times more permeant than Cs^+, the least permeant cation. Examination of

the line of identity. The Na^+ value of 0.28, the Li^+ value of 0.23, and the Cs^+ value of 0.17 have been used in constructing the empirical isotherms for these ions, drawn by eye through all the points.) The observed regularity means that the same physical factor (probably site field strength or coordination number, increasing from right to left: *cf.* Diamond & Wright, 1969) determining P_{Rb}/P_K determines the permeabilities of the other cations; this regularity also means that, therefore, once one knows the permeabilities of two cations, one not only can predict qualitatively the whole alkali-cation sequence but also quantitatively the approximate relative permeabilities of the other three cations. The degeneracy of the abscissa and the maxima in the isotherms mean that a given P_{Rb}/P_K may correspond to either of two sequences and relative permeabilities. The intersections of these five experimental isotherms determine transitions between different selectivity sequences. The first four sequences and the eleventh sequence, reading from right to left, are those predicted from a purely Coulomb model of selectivity; sequences 5 through 10 differ from Coulomb predictions only in the higher potency of Li^+; and the last three or "post-Coulomb" sequences may involve polarization of the largest cations by the sites (*see* pp. 371–375 of text, and pp. 581–607 of Diamond & Wright, 1969, for further discussion)

so-called empirical selectivity isotherms for biological systems (Eisenman, 1965, Fig. 8) shows that systems exhibiting sequence V or VIa usually exhibit a total selectivity range of about 50:1. In order to determine whether low selectivity magnitudes are peculiar to the gallbladder or are a general characteristic of epithelia, we have tentatively constructed, in Fig. 7, alkali-cation selectivity isotherms based solely on measurements of transepithelial potentials in epithelial preparations (rabbit and frog gallbladders, rabbit and frog intestines, frog choroid plexus, inside and outside surfaces of bullfrog and leopard-frog skins, serosal and mucosal surfaces of toad urinary bladder). These isotherms express the fact that not only are there qualitative regularities in epithelial permeability (i.e., only a few of the 120 possible permutations of the alkali cations are observed as permeability sequences), but there are also quantitative regularities: a given sequence is associated only with a certain range of permeability ratios, and knowledge of one permeability ratio permits prediction of permeability ratios for the other cations. The legend for Fig. 7 of this paper, and Figs. 1 and 2 of Diamond and Wright, 1969, give further details of the construction and interpretation of selectivity isotherms.

The following two conclusions emerge from comparison of the epithelial isotherms of Fig. 7 with the general biological isotherms previously constructed by Eisenman (1963, Fig. 3, and 1965, Fig. 8) and based mainly on membranes of single cells such as nerve, muscle, erythrocytes, yeast, algae, and bacteria.

(1) The epithelial isotherms lie closer together than do Eisenman's: i.e., a small range of selectivity is a general characteristic of transepithelial ion permeation. In no epithelium, to our knowledge, does the permeability range from the least-permeable to the most-permeable alkali cation exceed a factor of 23, and the range is less than a factor of 2 in several epithelia. In contrast, a range of a factor of about 50 is typical for single cells. The range of selectivity in a membrane depends upon its degree of hydration (Eisenman, 1961: *cf.* Fig. 6; Diamond & Wright, 1969, p. 608), high hydration being associated with low selectivity. This suggests that the high-conductance pathway for ion permeation across epithelia is more hydrated than the pathway across most single-cell membranes, as a result of epithelia being specialized to carry out high rates of water transport (Diamond, 1964). Analysis of nonelectrolyte permeation also suggests that the route of permeation through gallbladder epithelium is relatively highly hydrated (Smulders & Wright, 1971). A possible structural basis for this finding will be discussed on pp. 389–390.

(2) The Li^+ isotherm in epithelia is shifted down in its relative position, so that Li^+ is relatively more permeant in epithelia than in most single cells. Instances in which Li^+ is more permeant than predicted from a purely Coulomb model of ion:site interactions arise not only in rabbit gallbladder but also at the inside surface of bullfrog skin, the inside surface of leopard-frog skin, and the serosal surface of toad urinary bladder. This suggests that the class of molecules controlling cation permeation in epithelia may differ from those in most single cells and may be more polarizable.

Anion Permeation

Dilution potentials for a 2:1 NaCl concentration gradient (1.88:1 activity gradient) measured within a few minutes of dissection yield values of at least 13.2 mV. These early values decline rapidly with time (*cf.* Fig. 5), so that by extrapolation the values that would be recorded *in vivo* must be higher. Even the value of 13.2 mV is close to the theoretical Nernst value (16.1 mV) for this gradient in a perfectly cation-selective membrane and corresponds to a calculated value of P_{Cl}/P_{Na} of 0.08 or less. By the end of 1 or 2 hr after dissection, at a time when most of the experimental measurements analyzed in this paper were obtained, the 2:1 NaCl dilution potential has usually decreased on the average to 8 mV, yielding a calculated P_{Cl}/P_{Na} of 0.33. This increase in anion permeability is due to the development of something approximating a free-solution shunt (pp. 370 and 381). Thus, nearly all of the anion permeation under our experimental conditions must be via shunt, not via native membrane. This conclusion is supported by estimates of the temperature dependence of anion conductance. From 4 to 37 °C, P_{Cl}/P_{Na} in the gallbladder declines from 0.39 to 0.09 (Machen & Diamond, 1969), while membrane conductance increases by 3.3 times (E. M. Wright, *unpublished observation*). From these figures, one may calculate a Q_{10} of 1.72 for Na^+ conductance but only 1.13 for Cl^- conductance. The latter value does not differ significantly from the Q_{10} for the limiting equivalent conductivity of Cl^- in free solution, 1.25 (Robinson & Stokes, 1965).[2]

---

2 Cl^- and Br^- exhibit "exchange diffusion" in the gallbladder; i.e., the one-way tracer fluxes of halides are an order of magnitude larger than predicted from electrical measurements (Diamond, 1962; Wheeler, 1963). This implies that the gallbladder membrane contains a positively charged carrier (mobile ion exchanger) with which anions associate to yield an electrically neutral complex but which produces no net anion flux, hence no electrical manifestations and no effects in any of the present experiments. The exchange-diffusion mechanism may reside in some membrane other than the transepithelial high-conductance pathway, e.g., in the cell membranes rather than in the tight junctions.

There are two possible reasons why the anion permeability of the native membrane is so much lower than the cation permeability. (1) The membrane may contain many fewer Cl^- ions than cations, either because it has fixed anionic groups balanced by mobile cations, or because it is thin enough for microscopic electroneutrality to be violated and contains an excess of cations owing to the presence of neutral cation-sequestering molecules. (2) The membrane may contain equal numbers of Cl^- ions and cations, but the Cl^- ions may have a much lower mobility. The latter explanation appears to be the correct one (pp. 376–381).

The Cation Permeation Mechanism

(*1*) *The Membrane is Thick Enough that Microscopic Electroneutrality has to be Obeyed.* As discussed in paper III, this conclusion follows from the fact that the current-voltage relation is linear both in symmetrical solutions and in the presence of a single-salt concentration gradient. In membranes thin enough that microscopic electroneutrality is violated, the current-voltage relation is nonlinear in both cases if the ion actually passes into the low-dielectric membrane region, and is nonlinear in the case of a single-salt concentration gradient if the ion traverses the membrane via a polar pore (e.g., by a chain of fixed neutral sites: *see* paper II).

(*2*) *The Sites Controlling Cation Permeation are Neutral, i.e., Lack Net Charge.* (*a*) Two experiments discussed in paper III, *viz.*, the linear conductance-concentration relation and the only slight concentration dependence of the anion/cation permeability ratio, showed that cation permeation in the gallbladder is not via charged cation-exchange sites, whether mobile or fixed. (*b*) Fig. 2 (compare experimental points with the theoretical curve "cation-exchanger-plus-shunt") showed that fixed charged sites fit poorly the experimental relation between dilution potentials and concentration gradient. Mobile charged sites would give an identically poor fit, since potential-concentration relations are the same for fixed and mobile charged sites (Conti & Eisenman, 1966). (*c*) If there were mobile charged sites with tightly associated counter-ions, cation permeability estimated with radioactive tracers would exceed that measured electrically ("exchange diffusion"), but this is not the case for Na^+ and K^+ (Diamond, 1962; Wheeler, 1963; Diamond, 1968). (*d*) If there were mobile charged sites with dissociated counter-ions, the current-voltage curves would be nonlinear (Conti & Eisenman, 1966), but the observed curves are linear. (*e*) Finally, it is difficult to reconcile any type of ion exchanger with the experimental results concerning cation selectivity sequences. Four different kinds of measurements – conductances (paper III, p. 343), the Ca^{++} effect (paper III, p. 354),

dilution potentials (this paper, Table 4a, p. 386), and biionic potentials (this paper, Table 4b, p. 386)—yield essentially the same permeability sequence, $K^+ > Rb^+ > Na^+ > Li^+ > Cs^+$, with uncertainty only concerning the relative positions of Li^+ and Cs^+ owing to the effect of the shunt. As discussed in paper III, permeability coefficients depend upon some combination (the exact form depending on the permeation mechanism) of an equilibrium factor, such as a binding constant, times a non-equilibrium factor, such as a mobility. Since these factors are determined by different forces, the ion mobility sequence will almost always differ from the equilibrium selectivity sequence in the same membrane. The Ca^{++} effect in the gallbladder is presumed to measure the equilibrium selectivity sequence uninfluenced by mobility differences (paper III, p. 354). In the case of an ion-exchange membrane (Teorell, 1953; Conti & Eisenman, 1965), the permeability sequence as measured either by dilution potentials or by conductances becomes identical to the mobility sequence and is uninfluenced by the equilibrium factor, whereas the permeability coefficient measured by biionic potentials is proportional to the product of the equilibrium binding constant times the mobility. Thus, the finding in the gallbladder that the Ca^{++} effect, dilution potentials, conductances, and biionic potentials all give the same selectivity sequence is not a result expected for an ion exchanger.

(*3*) *The Neutral Sites Controlling Cation Permeation are Probably Fixed, not Mobile.* Given the conclusions that the membrane is thick enough to obey microscopic electroneutrality and that the sites controlling cation permeation lack net charge, two alternative physical mechanisms may be suggested: either the sites are fixed within a polar pore, or the sites are mobile within a hydrocarbon-like membrane (a model would be valinomycin or monactin in a bulk hexane-phase membrane between two aqueous phases).

The following reasoning, based on the low anion permeability of the native membrane, makes it more probable (but not certain) that fixed sites are the correct interpretation. If there are fixed dipolar sites lining a neutral pore, then the low P_{Cl} (at least 12 times less than P_{Na}) might be attributed to low anion mobility owing to the negative ends of the dipoles protruding towards the center of the pore. However, it is more difficult to provide a physically realistic picture of a thick, hydrocarbon-like membrane containing neutral carriers for cations but with low anion permeability.[3] The

3 If such a membrane is thin enough to violate microscopic electroneutrality, anion permeability is zero simply because the membrane contains no anions (Szabo, Eisenman & Ciani, 1969).

electroneutrality condition requires that the membrane contain as many anions as there are cation-carrier complexes. The free halides would be virtually insoluble in hydrocarbon and would themselves require a lipid soluble neutral carrier (e.g., cation extraction from water into a monactin containing hexane phase is immeasurably low if the only available anion is Cl^-, and requires a lipid-soluble anion such as picrate to be detectable Eisenman, Ciani & Szabo, 1969). For the anion mobility to be much lower than the cation mobility, this suggests an anion carrier much larger than the cation carrier. Yet known cation carriers, such as valinomycin, monactin and cyclic polyethers, are substances with molecular weights of 1,000 or more To explain P_{Cl} at least 12 times lower than P_{Na}, the anion carrier would require a molecular weight of a least 144,000, assuming diffusion coefficient to vary as the inverse square root of molecular weight. Although the possibility of such a large, lipid-soluble, anion carrier cannot be excluded, a fixed-site mechanism obviating the necessity of this postulate seems more plausible. In addition, the sum of the evidence (pp. 389–391) suggests that permeation in the gallbladder is not via a typical hydrocarbon-like cell membrane but via some relatively hydrated channel, where a carrier seems unlikely.

(*4*) *Evidence for the Model of a Thick Membrane with Fixed Neutral Site plus a Shunt.* The permeation model that appears most readily compatible with our experimental results is represented in Fig. 8. A membrane thick enough that microscopic electroneutrality is obeyed is traversed by chains of dipolar sites constituting polar "pores", which contain equal numbers of mobile cations and mobile anions from the bathing solution. The negative ends of the dipoles point toward the center of the channel, so that anions have a much higher electrochemical potential, and perhaps a much lower mobility, than cations and hence a negligible permeability in this channel. In parallel with these channels are some free-solution shunts, which account for the low but measurable anion conductance of the membrane. Since the anion and cation conductances of the shunt are in the ratios of the free solution mobilities, most of the total membrane cation conductance arises from the dipolar channel. A detailed quantitative treatment of this permeation mechanism, including the non-ideal activity factor n (pp. 383–385) as a parameter, is given in paper II, model 2.

This model correctly accounts for the main features of ion permeation in the gallbladder: current-voltage curves are predicted to be linear, both in symmetrical solutions and in the presence of a single-salt concentration gradient [paper II, Eq. (58)].

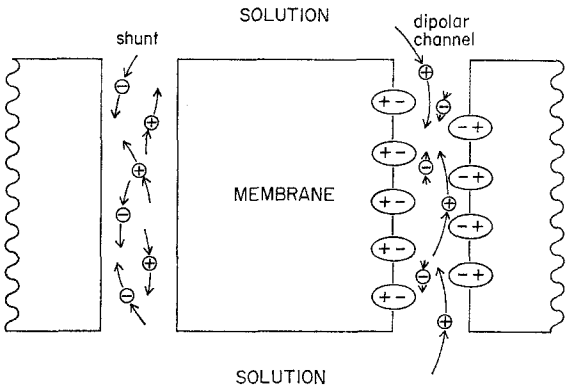

Fig. 8. Reconstruction of ion permeation mechanism in gallbladder epithelium. A section of epithelial membrane (probably the tight junction) is traversed by channels lined with dipolar groups (e.g., $\delta+\rangle C=O\ \delta-$), whose negative ends point into the channels. The numbers of cations (symbolized by ⊕) and anions (symbolized by ⊖) in the channels are equal. However, mobilities (indicated by lengths of arrows) might be higher for cations than for anions, since the ions are migrating in a predominantly negative environment and thus cations and anions might be compelled to move in paths differing in their detailed geometry and length, depending on the configuration of the channel and the dipoles. In parallel with the dipolar channels are shunts in which cations and anions move with free-solution mobility ratios

The conductance-concentration relation is predicted to be linear if $n=1$ [paper II, Eq. (60)]. A value of $n \neq 1$ tends to make the relation nonlinear (supralinear if $n<1$, sublinear if $n>1$). However, the deviation from linearity predicted for the gallbladder (for the measured values of $n=0.8$ and of shunt conductance) is small and falls within the experimental error of the conductance measurements.

The anion/cation permeability ratio shows little dependence on ionic strength, because the conductance-concentration relation is linear for the shunt and nearly linear for the dipolar channel.

There is no exchange diffusion of cations (i.e., estimates of cation conductance from electrical measurements and from radioactive tracer fluxes agree), because cations are not moving in association with a negatively charged carrier.

The equation derived from this model [paper II, Eq. (53)] gives a good quantitative fit to the experimentally determined relation between dilution potentials and concentration gradient (Fig. 2), using a value of n close to that determined by a different type of experiment (p. 384).

The model correctly predicts that measurements of conductance and of permeability coefficients based on dilution potentials should yield the same

cation selectivity sequence if n is close to 1, since exactly the same function $[u_1(K_1K_3)^{1/2n}]$ of the equilibrium constants K and the mobilities u appears in both expressions [paper II, Eqs. (53) and (58)]. As discussed on p. 382, the form of the equations combined with experimental limitations has unfortunately made it impossible to extract values of gallbladder K's and u's from the experimental data by means of the equations, or to demonstrate that permeability coefficients based on biionic potentials and on dilution potentials should have the same sequence and values. However, the latter prediction can be demonstrated to follow from the similar but less complex equations describing a thin membrane with fixed neutral sites plus shunt (paper II, model 4), and it seems likely by analogy that the prediction will be approximately valid for the case of a thick membrane (*see* p. 383 for further discussion).

(*5*) *Effects of pH, Polyvalent Cations, and Ionic Strength on Permeation*
The permeability changes caused by these three agents in the gallbladder are reminiscent of their effects on ion exchangers but must have a different explanation, since the evidence is compelling that the gallbladder is not an ion exchanger (pp. 376–377).

Lowering the pH, or raising the concentration of polyvalent cations such as Ca^{++} or Th^{+4}, reversibly converts the gallbladder (Wright & Diamond, 1968; Machen, 1970; paper III) and barnacle muscle (Hagiwara, Toyama & Hayashi, 1971) from being preferentially cation-permeable to being preferentially anion-permeable, by simultaneously lowering cation conductance and increasing anion conductance. These findings were initially interpreted in terms of an ion-exchange permeation mechanism, since similar observations have often been reported for ion-exchange membranes where protonation may convert negatively charged sites for cation exchange (e.g., carboxyls) into neutral groups while converting other neutral groups (e.g., amines) into positively charged sites for anion exchange, and thus may alter the relative *numbers* of mobile cations and anions. However, these effects may also be expected to arise in thick membranes with fixed neutral sites, where the number of mobile cations necessarily equals the number of mobile anions but where these three agents may act by changing the cation/anion mobility ratio. If a channel is lined with dipolar groups whose negative ends point toward the channel lumen, association of H^+ or polyvalent cations with the negative ends will change the environment in which ions migrate from a predominantly negative one to a positive one, and may thus depress cation mobility while raising anion mobility. Effects of pH and polyvalent cations similar to those in the gallbladder have been observed in

two other epithelia in which ion permeation appears to be controlled by fixed neutral sites (E. M. Wright, *unpublished observations*), namely, intestine (Smyth & Wright, 1966) and choroid plexus (Wright & Prather, 1970).

A related phenomenon in the gallbladder may be the slight increase in the P_{Cl}/P_{Na} ratio with increasing ionic strength (paper III, Fig. 8), which is definitely outside the range of experimental error, although much slighter than would be found for an ion exchanger. With increasing ionic strength in the gallbladder, Na^+ may associate with the negative ends of an increasing fraction of the dipoles and depress cation mobility relative to anion mobility in the same way that H^+ and Ca^{++} are postulated to do.[4]

Mathematical Analyses of Permeation

In this section we analyze the p.d. measurements by means of the equations, derived in paper II, model 2, describing a thick membrane with fixed neutral sites and a shunt. Permeability coefficients will also be calculated for comparison by means of several other equations, in order to illuminate the significance of the differences between these equations.

(*1*) *Treatment of the Shunt.* The approach of relative permeability coefficients (henceforth referred to as *P*'s) in the gallbladder toward free-solution mobility ratios with time after dissection could be approximated for mathematical purposes in either of two ways: (a) by assuming the existence of a single channel in which conductance increases and *P*'s change with time and through which both cations and anions permeate; or (b) by assuming a native membrane channel with time-invariant properties (constant conductance, constant *P*'s for cations, zero mobility for anions) in parallel with a channel in which ionic *P* ratios equalled free-solution mobility ratios and whose conductance increased with time. We have adopted the latter solution for the following three reasons. First, the former hypothesis is equivalent to a thick membrane with fixed neutral sites and no shunt, treated mathematically in paper II, model 1. This model predicts, contrary to the experimental findings for the gallbladder, that different cation selectivity sequences should be obtained from dilution potentials [determined only by *u*'s, not by *K*'s: paper II, Eq. (42)], from biionic potentials

4 Still a third mechanism by which pH, polyvalent cations, and ionic strength may affect permeability appears in thin lipid membranes containing neutral carriers, where these agents produce effects very similar to those observed in thick ion exchangers and in thick fixed-neutral-site membranes. In this case, these agents act by altering surface charge and thus changing the work required to bring ions into a thin membrane in which microscopic electroneutrality is violated (Szabo *et al.*, 1969; McLaughlin, Szabo, Eisenman & Ciani, 1970).

[determined both by K's and u's: paper II, Eq. (43)], and from the Ca^{++} competition effect (determined only by K's). Secondly, the latter hypothesis (native-membrane channel plus shunt) agrees with the finding that the increases in Na^+ conductance and in Cl^- conductance with time do stand in the free-solution mobility ratios. Finally, the latter hypothesis accounts satisfactorily for the apparent changes in P_{Li}/P_{Na} and in P_{Cs}/P_{Na} with time, since both ratios become independent of time after correction for the shunt (p. 388 and Table 5). However, the shunt hypothesis still represents only an approximation to the real situation, since it accounts only in part for the apparent changes in P_K/P_{Na} and P_{Rb}/P_{Na} with time (p. 388 and Table 5).

Since dilution potentials recorded from gallbladders soon after dissection are close to the Nernst values for an anion-impermeable membrane and initially decline rapidly with time, we have assumed that anion mobility in the native-membrane channel (u_3 in paper II, model 2) is zero and that all Cl^- conductance is in the shunt.

(*2*) *Separation of K's and u's.* It would be interesting to calculate for each cation not only P, but also K and u separately. Unfortunately, this is impossible with the available experimental information for the gallbladder, using models with shunts. Both dilution potentials [paper II, Eq. (53)] and conductances [paper II, Eq. (58)] yield the same combination of the K's and u's, *viz.*, $u_1(K_1K_3)^{1/2n}$, so that K and u cannot be extracted separately. The same difficulty applies to the related model of a thin membrane with fixed neutral sites and shunt [paper II: the combination $u_1K_1^{1/n}$ appears in dilution potentials (Eq. 110), conductances (Eq. 107), and biionic potentials (Eq. 113)]. However, it may be recalled that the same cation selectivity sequence is obtained in the gallbladder from the Ca^{++} competition effect, a function only of the K's, as from dilution potentials, biionic potentials, and conductances, which are functions both of the K's and the u's (p. 377). This implies that in the gallbladder cation u ratios are much closer to 1 than are the K ratios, and that permeability ratios are close to K ratios, as also true in glass electrodes (Eisenman, 1967).

(*3*) *Analysis of Biionic Potentials.* With the available experimental information in the gallbladder, P's can be extracted from dilution potentials but not from biionic potentials by the thick-membrane equations of paper II model 2, since the biionic-potential equation for a thick membrane with shunt is too complex [paper II, Eq. (62)].

We have instead analyzed biionic potentials, and used them to extract the non-ideal activity factor n (*see* next section), by the equation describing a *thin* membrane with fixed neutral sites plus shunt [paper II, Eq. (113)]

If biionic permeability values could have been extracted from the thick-membrane equations, they would probably have been close to the values actually extracted by means of the thin-membrane equations, because: (a) P's extracted from dilution potentials by the thick-membrane equation [paper II, Eq. (53)] and the thin-membrane equation [paper II, Eq. (110)] agree within better than 2% (*compare* Tables 4a and b); and (b), in the absence of a shunt, the thin-membrane equation for biionic potentials [paper II, Eq. (99)] becomes identical in form to the Goldman-Hodgkin-Katz equation [Eq. (1)], which in turn yields very similar values (*compare* Tables 4e and f) to those extracted from the equation for a thick membrane without shunt, despite the latter's different and more complicated form [paper II, Eq. (43)].

(*4*) *The Non-ideal Activity Factor n.* P ratios calculated from biionic mixture potentials by means of the Goldman-Hodgkin-Katz equation were found to change with solution composition (Fig. 4 and p. 367). Similar apparent shifts in relative permeability ratios with biionic mixture composition have been observed in cation-selective glass electrodes and aluminosilicate ion exchangers. Eisenman (1962) showed that such shifts are to be expected theoretically: since ion activities in a membrane are in general proportional to the n^{th} power of ion concentrations and since this non-ideal activity factor n is expected from regular solution theory to be able to assume values other than 1.0 (Garrels & Christ, 1965; Doremus, 1969), the potential of a perfectly cation-selective anion-impermeant membrane should be given by an equation of the form

$$\Delta E=(RT/F)\ln([A^+]^{1/n}+K^{1/n}[B^+]^{1/n})^n$$

where $[A^+]$ and $[B^+]$ are the activities of cations A^+ and B^+, and K is the equilibrium-constant ratio for the two cations. This equation, with values of n which often differ from 1.0, does in fact empirically describe ion binding by aluminosilicate ion exchangers and the potentials of cation-selective glass electrodes. If experimental results are fitted to an equation assuming $n=1.0$ but if n actually is less than 1.0, then the calculated relative permeability of a cation will apparently increase with its mixture proportion, as in the gallbladder. Hence it seemed worthwhile to examine if use of an equation with n less than 1.0 to fit the gallbladder results yielded concentration-independent permeability ratios.

The measurements of biionic mixture potentials as a function of cation gradients were analyzed by the thin-membrane equation [paper II, Eq. (113)] (not by the thick-membrane equation, for the reasons discussed above).

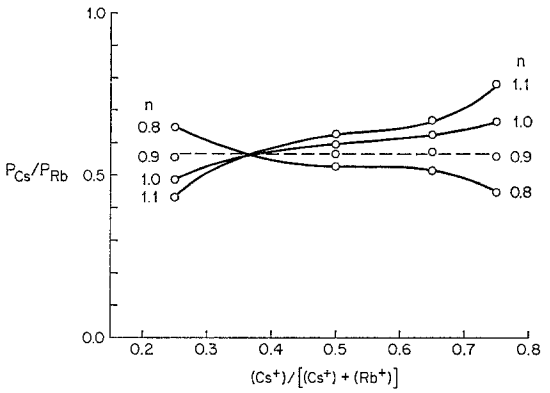

Fig. 9. Estimation of the non-ideal activity factor n for cation permeation in a gallbladder. Biionic potentials were measured in 150 mM salt solutions consisting of mixtures of RbCl and CsCl in various proportions. From the measured p.d.'s for each mixture, the permeability ratio $P_{Cs}/P_{Rb}=u_{Cs}K_{Cs}^{1/n}/u_{Rb}K_{Rb}^{1/n}$ was calculated from Eq. (113) of paper II for the model of a thin membrane with fixed neutral sites and a shunt, the calculation being carried out at four different values of n. The abscissa gives the average proportion of Cs^+ in the mucosal and serosal bathing solutions, the ordinate is the calculated P_{Cs}/P_{Rb}, and each curve represents the calculation for a different value of n indicated beside the curve. It is apparent that for this particular gallbladder the calculated P_{Cs}/P_{Rb} is virtually independent of solution composition for $n=0.9$ (the dashed horizontal line would correspond to complete independence) but varies systematically with solution composition for higher or lower values of n. The average value of n for all gallbladders studied was 0.8

The procedure was to calculate P ratios as a function of concentration gradient, using different values of n. In the experiment and calculations on Cs^+–Rb^+ biionic potentials illustrated in Fig. 9, the calculated ratio P_{Cs}/P_{Rb} was virtually independent of gradient when n was chosen as 0.9, but the calculated ratio increased with $(Cs^+)/[(Rb^+)+(Cs^+)]$ for higher values of n ($n=1.0$ or 1.1, Fig. 9), and decreased for lower values ($n=0.8$, Fig. 9). In five other experiments in which biionic potentials were measured as a function of gradient (four others involving the Rb^+–Cs^+ pair, one Na^+–K^+), it was also found necessary to choose a value of n less than 1.0 to obtain a P ratio independent of gradient. The average value of n for all six experiments was 0.8 ± 0.1. This conclusion is in good agreement with the quite independent evidence derived from analysis of dilution potentials as a function of gradient, which showed that a curve based on $n=1$ deviated somewhat from the experimental results and that a good fit was obtained by choosing $n=0.7$ (Fig. 2).

Thus, the apparent changes in cation permeability ratios with cation mixture proportions, as extracted from measured biionic mixture potentials

in the gallbladder by the Goldman-Hodgkin-Katz equation, are systematic changes described by a value of the non-ideal activity factor n differing from 1.0, as in many artificial systems. It is only a first approximation to take n as 0.8 for the gallbladder, since different ions may have different values of n in the same membrane (Eisenman, 1962). However, the value of n from our single Na^+–K^+ experiment and the average value from our five Rb^+–Cs^+ experiments are both 0.8.

The physical meaning of values other than 1 is that there is some kind of interaction between sites, such that the binding of an ion at one site alters the relative binding constants of ions at an adjacent site. Values of n greater than 1 correspond to decreases in affinity for a given ion as its mixture proportion increases, values less than 1 (as in the gallbladder) to increases in affinity. A system whose behavior resembles that of the gallbladder is the ammonium form of an aluminosilicate ion exchanger called permutit, in which the value of n is 0.67 for Cs^+–NH_4^+ exchange and 0.74 for H^+–NH_4^+ exchange (Eisenman, 1969, Fig. 3.9)—i.e., as an increasing fraction of the sites becomes occupied by H^+ or Cs^+, the remaining sites show an increasing preference for these ions over NH_4^+. The molecular basis of the cooperative phenomenon responsible for site interactions and for values of n other than 1 is unknown in the gallbladder, but in glass electrodes it appears to involve a swelling or shrinking of the glass lattice to accommodate a larger (or smaller) ion and resulting in an altered selectivity pattern.

(*5*) *Calculation of Permeability Coefficients.* For all the individual experiments listed in Table 1, P ratios were extracted from dilution potentials and from biionic potentials by each of six different equations. The average values of the P ratios obtained by each equation are listed in Table 4a–4e.

The P's obtained from the model of a thick membrane with fixed neutral sites plus shunt, $n=0.8$, are considered the most appropriate and physically realistic values (Table 4a), but values could be obtained only from dilution potentials (values for individual experiments are listed in Table 1, column 6), not from biionic potentials. The corresponding thin-membrane treatment, $n=0.8$ (Table 4b), yields identical P's from dilution potentials. The thin-membrane P's from biionic potentials (values for individual experiments are listed in Table 1, column 7) stand in the same sequence as, and are in good quantitative agreement with, the P's from dilution potentials, except for the higher estimate of P_K from biionic potentials. Tables 4a and 4b also show that even in gallbladders in which a significant shunt has developed, P_{Li} exceeds P_{Cs} after correction for the shunt.

Table 4a. *Cation permeability ratios, calculated from the thick fixed-neutral-site model with shunt and $n=0.8$* [a]

Cation	Permeability relative to Na^+ from dilution potentials
K^+	2.4 $\pm$0.2
Rb^+	1.7 $\pm$0.4
Na^+	1.0
Li^+	0.74 $\pm$0.13
Cs^+	0.65 $\pm$0.09

[a] From the potential measurements of Table 1, average relative permeability coefficients were calculated as in Table 2, except that Eq. (53) of paper II was used, taking $u_3=0$ [P_{cation}/P_{Cl} calculated as $u_1(K_1K_3)^{1/2n}/\lambda_s A_n v_3$].

Table 4b. *Cation permeability ratios, calculated from the thin fixed-neutral-site model with shunt and $n=0.8$* [a]

Cation	Permeability relative to Na^+	
	From dilution potentials	From biionic potentials
K^+	2.4 $\pm$0.3	3.6 $\pm$0.3
Rb^+	1.7 $\pm$0.5	2.0 $\pm$0.8
Na^+	1.0	1.0
Li^+	0.74 $\pm$0.13	0.83 $\pm$0.08
Cs^+	0.65 $\pm$0.09	0.62 $\pm$0.07

[a] From the potential measurements of Table 1, average relative permeability coefficients were calculated as in Table 2, except that we used Eq. (110) of paper II for dilution potentials (P_{cation}/P_{Cl} calculated as $u_1K_1^{1/n}/\lambda_s v_3$) and Eq. (113) of paper II for biionic potentials (P_{cation}/P_{Na} calculated as $u_2K_2^{1/n}/u_1K_1^{1/n}$), taking $u_3=0$ in both cases.

Table 4c. *Cation permeability ratios, calculated from the thick fixed-neutral-site model with shunt and $n=1.0$* [a]

Cation	Permeability relative to Na^+ from dilution potentials
K^+	2.4 $\pm$0.2
Rb^+	1.7 $\pm$0.4
Na^+	1.0
Li^+	0.74 $\pm$0.13
Cs^+	0.65 $\pm$0.09

[a] From the potential measurements of Table 1, average relative permeability coefficients were calculated as in Table 4a, except that n was taken as 1.0.

Table 4d. *Cation permeability ratios, calculated from the thin fixed-neutral-site model with shunt and $n=1.0$* [a]

Cation	Permeability relative to Na^+	
	From dilution potentials	From biionic potentials
K^+	2.4 ±0.2	2.7 ±0.2
Rb^+	1.7 ±0.4	1.6 ±0.6
Na^+	1.0	1.0
Li^+	0.74±0.13	0.87±0.08
Cs^+	0.64±0.09	0.67±0.06

[a] From the potential measurements of Table 1, average relative permeability coefficients were calculated as in Table 4b, except that n was taken as 1.0.

Table 4e. *Cation permeability ratios, calculated from the thick fixed-neutral-site model with $n=1.0$ and no shunt* [a]

Cation	Permeability relative to Na^+	
	From dilution potentials	From biionic potentials
K^+	2.3 ±0.2	2.4 ±0.1
Rb^+	1.8 ±0.4	1.7 ±0.4
Na^+	1.0	1.0
Cs^+	0.87±0.10	0.89±0.01
Li^+	0.74±0.10	0.84±0.08

[a] From the potential measurements of Table 1, average relative permeability coefficients were calculated as in Table 2, except that we used Eq. (42) of paper II for dilution potentials (P_{cation}/P_{Cl} calculated as u_1/u_3) and Eq. (43) of paper II for biionic potentials (P_{cation}/P_{Na} calculated as $u_2K^{1/n}/u_1$).

Tables 4c and 4d are identical to Tables 4a and 4b, respectively, except that n was taken as 1.0 instead of 0.8. Comparison of Table 4a with 4c, and 4b with 4d, shows that the effect of this change in n on P's calculated from dilution potentials is trivial, the only change being in the last decimal place of P_{Cs} calculated from the thin-membrane model (Tables 4b & 4d). The reason for the slightness of the effect is that the dilution potentials from which P's were extracted were for 2:1 gradients, and Fig. 2 shows that dilution potential curves for different values of n (compare the curves ····· and ——) diverge increasingly for increasing gradients. Comparison of Table 4b with 4d shows, however, that the choice of n makes a non-trivial difference in P's extracted from biionic potentials, especially on P_K. The

Table 5. *Cation permeability ratios as a function of time*[a]

Cation	P	
	30 min	120 min
K^+	3.2 ±0.1	1.9 ±0.2
Rb^+	2.0 ±0.1	1.3 ±0.2
Na^+	1.0	1.0
Li^+	0.91±0.02	0.90±0.01
Cs^+	0.56±0.03	0.56±0.06

[a] Biionic potentials were measured as a function of time in two gallbladders (Fig. 5 depicts the results of one of these experiments). From the p.d.'s measured at 30 and 120 min, the permeability relative to that of Na^+ was calculated from the model of a thin fixed-neutral-site membrane with shunt and $n=0.8$ [paper II, Eq. (113), $u_2 K_2^{1/n}/u_1 K_1^{1/n}$]. The apparent time dependence of LiCl and CsCl potentials (Fig. 5) is completely removed by correction for the shunt, since calculated values of P_{Li} and P_{Cs} for the membrane are constant, but some apparent time dependence remains for P_K and P_{Rb}.

significance for studies of permeability in biological membranes is that failure to measure the value of n, and the tacit assumption that $n=1.0$, may lead to calculation of misleading permeability ratios.

Table 4e gives P's extracted from the model of a thick membrane with fixed neutral sites and $n=1$ but no shunt (paper II, model 1). This model yields "lumped" P's for both native gallbladder membrane and the shunt. In contrast, the thick-membrane-plus-shunt model yields P values for native membrane corrected for the presence of a shunt; hence P values are further from free-solution mobility ratios than are uncorrected P values. Comparison of Tables 4e and 4c shows that the most marked effect is on Cs^+, whose permeability relative to that of Na^+ is further removed from the free-solution value than that of any other ion. Correction for the shunt lowers P_{Cs} from 0.87 to 0.65 and reveals that Cs^+ is less permeant than Li^+. Shunt corrections are further illustrated in Table 5, which compares P ratios based on biionic potentials measured at 30 min and at 120 min after dissection and calculated from the thin-membrane-plus-shunt model with $n=0.8$. If the decline in p.d.'s with time toward free-solution junction potentials (Fig. 6) was solely due to the development of a free-solution shunt, then P's in native membrane corrected for the effect of the shunt, as in Table 5, should be independent of time. Table 5 shows that P_{Li} and P_{Cs} both remain constant between 30 and 120 min, but P_K and P_{Rb} do not. Thus, a model invoking a free-solution shunt is an approximation but not a perfect representation of what is occurring in the gallbladder.

Finally, P ratios extracted from the Goldman-Hodgkin-Katz equation are listed in Table 2, which may be compared with the P ratios in Table 4e for the thick fixed-neutral-site membrane without shunt. The ratios differ only by one part in the second decimal place, a remarkable agreement between two equations of very different form.

Possible Structural Bases of the Permeation Mechanism

It will be recalled (paper I, Fig. 1) that gallbladder epithelium consists of a single sheet of cells; that each cell is attached to its neighbors around the entire periphery of its apex by a hoop-like tight junction, where the cell membranes from adjacent cells appear to fuse; and that the high-conductance pathway for transepithelial ion permeation might be, *a priori*, either across the tight junctions or else transcellular (across one epithelial cell membrane into the cell and out the opposite cell membrane). The following experimental findings argue strongly in favor of the tight-junction route:

(1) The current-voltage relation is linear in both symmetrical and asymmetrical single-salt solutions, a finding which is characteristic of a membrane thick enough to have to obey microscopic electroneutrality. In contrast, the current-voltage relation of thin lipid membranes is nonlinear (Szabo *et al.*, 1969; Neumcke & Läuger, 1969; Cass, Finkelstein & Krespi, 1970). This difference suggests that the main barrier to ion permeation in the gallbladder is considerably thicker than a thin lipid membrane or than a typical cell membrane. Since electron micrographs show the membranes of gallbladder epithelial cells to be of a thickness typical for cell membranes (ca. 80 Å) but the membrane-fusion region of the tight junctions to be ca. 2,000–3,000 Å thick (Tormey & Diamond, 1967), the observed current-voltage relation would be hard to reconcile with the transcellular route but is the one expected for the tight-junction route.

(2) Ion selectivity ratios in the gallbladder are nearer unity than in most single-cell membranes. Since low selectivity in model systems is associated with a high degree of hydration, this suggests that the route of transepithelial ion permeation in the gallbladder is more "watery" than in the usual cell membrane (p. 374). Analysis of nonelectrolyte selectivity also suggests a "watery" route of nonelectrolyte permeation (Smulders & Wright, 1971). Electron-microscopic observations of gallbladder tight junctions (J. M. Tormey, *personal communication*) reveal that the outer leaflets of the apposed plasma membranes are not fused throughout the entire length of the junction, but that instead there is a series of fusion sites between which the

membranes are separated for short distances by very narrow, presumably aqueous, spaces. The pattern is somewhat similar to that recently described for the tight junctions which seal off bile canaliculi (Goodenough & Revel, 1970). Thus, it is possible that these narrow spaces provide a network of tortuous aqueous channels from one end of the tight junction to the other, so that ions might be able to cross gallbladder epithelium without ever entering membrane lipid. The ultrastructure of the tight junctions would thus be correlated with the "watery" selectivity magnitudes of gallbladder epithelium compared to single cell membranes. Dipolar groups in the walls of the channels, such as carbonyls whose negative oxygen ends pointed into the channel, would serve as the sites responsible for permeability differences among ions.

(3) The symmetry of gallbladder permeability properties is the immediate expectation for a single membrane, such as the tight junction, but it is not generally expected for a series system of two membranes separated by a reservoir such as a cell (Sandblom & Eisenman, 1967), unless the two membranes happen to have the same relative permeability coefficients.

(4) The lack of effect of osmotic alteration of intracellular ion concentrations on transepithelial diffusion p.d.'s (paper I) suggests that the permeation route bypasses the cells.

(5) The effect of serosal concentration changes on transepithelial diffusion p.d.'s resulting from mucosal concentration changes agrees quantitatively with predictions based on a single membrane such as the tight junction and disagrees with predictions based on the transcellular route (paper I).

(6) Finally, the electrical resistance of the epithelial cell membranes, as determined by cable analysis of microelectrode recordings, is much higher than the transepithelial resistance (E. Frömter, *personal communication*). Thus, the high-conductance route for transepithelial ion permeation must bypass the cells.

For these reasons, the permeation mechanism studied in these papers probably resides in the tight junctions.

The nature of the shunt for ion permeation that develops with time after dissection is uncertain. It cannot be attributed to damaged tissue around the edge of a gallbladder sheet clamped between two chambers since the conductance per unit area is the same for a 2.6 mm^2 sheet as for a 1.13 cm^2 sheet, and since similar properties are observed for sheets as for cannulated intact gallbladder sacs with no cut edge. In light micrographs and electron micrographs, gallbladders several hours after dissection still

show few or no signs of damage that could give rise to a shunt, such as denuded epithelial cells, broken tight junctions, or widened gaps in tight junctions. The fact that there is no increase in sucrose permeability despite the conductance increase (Smulders, 1970) implies that the postulated shunt is permeable to ions but not to sucrose, that it cannot consist of gross holes or even fine pores, and that it more likely arises from changes in wall charges or dipoles along the route of ion permeation.

Some of the distinctive features of ion permeation in the gallbladder, which we associate with tight junctions, appear in other epithelia which resemble the gallbladder in having tight junctions and being specialized for isotonic fluid transport. Rabbit intestine and frog choroid plexus exhibit linear conductance-concentration relations and linear current-voltage relations (Schultz, Curran & Wright, 1967; E. M. Wright, *unpublished observations*). Low cation selectivity magnitudes for transepithelial permeation characterize many epithelia (Fig. 7). Thus, the cation permeation mechanism of the gallbladder may be relevant to other fluid-transporting epithelia.

Appendix

Fixed-Site Cation Exchanger in Parallel with Free-Solution Shunt

The membrane is assumed to contain ion-exchange channels with negative fixed charges and to be permeable only to cations, in parallel with and electrically insulated from free-solution shunts. The effective areas of the cation channel and of the shunt channel are written as ρ_c and ρ_s, respectively. Activities are symbolized by a, activity coefficients by γ, concentrations by C, fluxes by J, electrical potentials by ψ, and the Faraday by F. The membrane lies in a plane perpendicular to the x axis and extends from $x=0$ to $x=d$. Superscripts $'$ and $''$ refer to the two bathing solutions. Consideration is restricted to solutions containing only a single cation (subscript 1) and a single anion (subscript 3) (i.e., $a_1''=a_3''\equiv a''$, $a_1'=a_3'\equiv a'$), since in this paper (p. 362, Fig. 2) we shall use this model for calculation only of dilution potentials, not of biionic potentials. We make the following assumptions.

(1) There is perfect stirring on either side of the membrane, so that the bathing solutions have the composition of bulk solution right up to the membrane-solution interface.

(2) Activity-concentration relations in the membrane are ideal; i.e., the non-ideal activity factor n (*cf.* p. 383) equals 1, and $a_i=\gamma_i C_i$.

(3) Within the membrane, $d\gamma_i/dx=0$.

(4) Microscopic electroneutrality is obeyed throughout the membrane.

(5) Ion mobilities are represented by u_i in the cation channel, by v_i in the shunt channel. It is assumed that $dv_i/dx\sim 0$ for all ions.

Other assumptions regarding the cation channel are the same as those made by Conti and Eisenman (1965) in their treatment of ion exchangers.

To solve for the membrane potential at zero current, E_0, we shall calculate the cation flux in the cation channel (represented by J_1), then the difference between the

anion and cation fluxes through the shunt channel ($J_3 - J_1$), and finally we shall equate these two flux expressions.

On one hand, the flux in the cation channel has been calculated by Conti and Eisenman [1965, Eq. (49)] and reduces to the expression

$$J_1 = \frac{-\rho_c F}{S^+}\left[E + \frac{RT}{F}\ln\frac{a''}{a'}\right] \tag{2}$$

where S^+ is defined as equal to $\int_0^d dx/[u_1(x)\, C_0^+(x)]$, and $C_0^+(x)$ is the concentration of negatively charged sites in the cation channel. The total membrane voltage E is related to the applied voltage across the membrane E^* and the voltage for zero current across the membrane E_0 by

$$E^* + E^0 = E. \tag{3}$$

On the other hand, the relation between the ion fluxes in the shunt channel (identified as J_1^* and J_3^*) and the potential may be derived as follows. One starts from the Nernst Planck flux equations:

$$J_1^* = -\rho_s v_1\left[RT\frac{dC(x)}{dx} + FC(x)\frac{d\psi(x)}{dx}\right], \tag{4}$$

$$J_3^* = -\rho_s v_3\left[RT\frac{dC(x)}{dx} - FC(x)\frac{d\psi(x)}{dx}\right]. \tag{5}$$

Dividing Eqs. (4) and (5) by v_1 and v_3, respectively, adding, and integrating across the membrane yields:

$$\frac{J_1^*}{v_1} + \frac{J_3^*}{v_3} = \frac{2\rho_s RT}{x}[C(0) - C(x)]. \tag{6}$$

Subtracting Eq. (5) from Eq. (4), substituting expressions for $C(x)$ and dC/dx obtained from Eq. (6) and integrating across the membrane yields:

$$E = \psi'' - \psi' = \frac{\left[(v_3 - v_1)\left(\frac{J_1^*}{v_1} + \frac{J_3^*}{v_3}\right) + 2(J_1^* - J_3^*)\right]\frac{RT}{F}\ln\frac{a''}{a'}}{(v_1 + v_3)\left(\frac{J_1^*}{v_1} + \frac{J_3^*}{v_3}\right)}. \tag{7}$$

Continuity of the electrochemical potential and the electrical potential across the membrane-solution interfaces has been assumed for the shunt channel.

For both channels in parallel with no net current, the ion fluxes may be equated ($J_1 = J_3^* - J_1^*$), and by combining Eqs. (2), (6), and (7) one obtains for the p.d. at zero current E_0, after rearranging:

$$E_0 = \frac{(v_3 - v_1)(a'' - a') - \rho\beta^+\gamma\ln(a''/a')}{(v_3 + v_1)(a'' - a') + \rho\beta^+\gamma\ln(a''/a')}\frac{RT}{F}\ln(a''/a') \tag{8}$$

where $\beta^+ \equiv d/S^+$, d is the membrane thickness, and

$$\rho \equiv \frac{\rho_c}{\rho_s} = \frac{\text{area of cation channel}}{\text{area of shunt channel}}.$$

As $\rho \to 0$, corresponding to a large shunt, Eq. (8) becomes identical to the modified Henderson-Planck junction potential equation derived in paper I of this series [Eq. (1)].

References

Barry, P. H., Diamond, J. M. 1970. Junction potentials, electrode standard potentials, and other problems in interpreting electrical properties of membranes. *J. Membrane Biol.* **3**:93.

— — 1971. A theory of ion permeation through membranes with fixed neutral sites. *J. Membrane Biol.* **4**:295.

Bungenberg de Jong, H. G. 1949. Reversal of charge phenomena, equivalent weight and specific properties of the ionised groups. *In:* Colloid Science, vol. 2. H. R. Kruyt, editor. p. 259. Elsevier, New York.

Cass, A., Finkelstein, A., Krespi, V. 1970. The ion permeability induced in thin lipid membranes by the polyene antibiotics nystatin and amphotericin B. *J. Gen. Physiol.* **56**:100.

Conti, F., Eisenman, G. 1965. The steady-state properties of an ion exchange membrane with fixed sites. *Biophys. J.* **5**:511.

— — 1966. The steady-state properties of an ion exchange membrane with mobile sites. *Biophys. J.* **6**:227.

Diamond, J. M. 1962. The mechanism of solute transport by the gall-bladder. *J. Physiol.* **161**:474.

— 1964. The mechanism of isotonic water transport. *J. Gen. Physiol.* **48**:15.

— 1968. Transport mechanisms in the gall-bladder. *In:* Handbook of Physiology: Alimentary Canal, vol. 5, p. 2451. American Physiological Society, Washington.

— Wright, E. M. 1969. Biological membranes: The physical basis of ion and nonelectrolyte selectivity. *Ann. Rev. Physiol.* **31**:581.

Doremus, R. H. Ion exchange in glasses. *In:* Ion Exchange, vol. 2. J. A. Marinsky, editor. p. 1. Dekker, New York.

Eisenman, G. 1961. On the elementary atomic origin of equilibrium ionic specificity. *In:* Symposium on Membrane Transport and Metabolism. A. Kleinzeller and A. Kotyk, editors. p. 163. Academic Press, New York.

— 1962. Cation selective glass electrodes and their mode of operation. *Biophys. J.* **2**; Part 2:259.

— 1963. The influence of Na, K, Li, Rb, and Cs on cellular potentials and related phenomena. *Bol. Inst. Estud. Méd. Biol.* **21**:155.

— 1965. Some elementary factors involved in specific ion permeation. *In:* Proc. 23rd Intern. Congr. Physiol. Sci., Tokyo. p. 489. Excerpta Med. Found., Amsterdam.

— 1967. The origin of the glass-electrode potential. *In:* Glass Electrodes for Hydrogen and other Cations. G. Eisenman, editor. p. 133. Dekker, New York.

— 1969. The ion exchange characteristics of the hydrated surface of Na^+ selective glass electrodes. *In:* Glass Microelectrodes. M. Lavallée, O. Schanne, and N. C. Hébert, editors. p. 32. Wiley, New York.

— Ciani, S., Szabo, G. 1969. The effects of the macrotetralide actin antibiotics on the equilibrium extraction of alkali metal salts into organic solvents. *J. Membrane Biol.* **1**:94.

Garrels, R. M., Christ, C. L. 1965. Solutions, Minerals, and Equilibria. Harper and Row, New York.

Goldman, D. E. 1943. Potential, impedance, and rectification in membranes. *J. Gen. Physiol.* **27**:37.

Goodenough, D. A., Revel, J. P. 1970. A fine structural analysis of intercellular junctions in the mouse liver. *J. Cell Biol.* **45**:272.

Hagiwara, S., Toyama, K., Hayashi, H. 1971. Mechanisms of anion and cation permeation in the resting membrane of a barnacle muscle fiber. *J. Gen. Physiol.* (*in press*).

Hodgkin, A. L., Katz, B. 1949. The effect of sodium ions on the electrical activity of th giant axon of the squid. *J. Physiol.* **108**:37.

Leb, D. E., Hoshiko, T., Lindley, B. D. 1965. Effects of alkali metal cations on th potential across toad and bullfrog urinary bladder. *J. Gen. Physiol.* **48**:527.

Lindley, B. D., Hoshiko, T. 1964. The effects of alkali metal cations and commo anions on the frog skin potential. *J. Gen. Physiol.* **47**:749.

Machen, T. E. 1970. Anion Selectivity and Permeation Mechanism in Rabbit Gall bladder Epithelium. Ph. D. Dissertation, University of California at Los Angeles

— Diamond, J. M. 1969. An estimate of the salt concentration in the lateral intercellula spaces of rabbit gall-bladder during maximal fluid transport. *J. Membrane Bio* **1**:194.

McLaughlin, S. G. A., Szabo, G., Eisenman, G., Ciani, S. 1970. The effects of surfac charge on the conductance of phospholipid membranes. *Proc. Nat. Acad. Sci. 67* 1268.

Neumcke, B., Läuger, P. 1969. Nonlinear electrical effects in lipid bilayer membranes II. Integration of the generalized Nernst-Planck equations. *Biophys. J.* **9**:1160

Robinson, R. A., Stokes, R. H. 1965. Electrolyte Solutions. Butterworths, London.

Rothstein, A., Demis, C. 1953. The relationship of the cell surface to metabolism. Th stimulation of fermentation by extracellular potassium. *Arch. Biochem. Biophys* **44**:18.

Sandblom, J. P., Eisenman, G. 1967. Membrane potentials at zero current: the signifi cance of a constant ionic permeability ratio. *Biophys. J.* **7**:217.

Schultz, S. G., Curran, P. F., Wright, E. M. 1967. Interpretation of the hexose-depend ent electrical potential differences in small intestine. *Nature* **214**:509.

Smulders, A. P. 1970. The Permeability of the Gall-Bladder to Non-Electrolytes. Ph. D Dissertation, University of California at Los Angeles.

— Wright, E. M. 1971. The magnitude of non-electrolyte selectivity in the gallbladde epithelium. *J. Membrane Biol.* (*in press*).

Smyth, D. H., Wright, E. M. 1966. Streaming potentials in the rat small intestine *J. Physiol.* **182**:591.

Szabo, G., Eisenman, G., Ciani, S. 1969. The effects of the macrotetralide actin anti biotics on the electrical properties of phospholipid bilayer membranes. *J. Membran Biol.* **1**:346.

Teorell, T. 1953. Transport processes and electrical phenomena in ionic membranes *Prog. Biophys. Biophys. Chem.* **3**:305.

Tormey, J. M., Diamond, J. M. 1967. The ultrastructural route of fluid transport ir rabbit gall bladder. *J. Gen. Physiol.* **50**:2031.

Wheeler, H. O. 1963. Transport of electrolytes and water across wall of rabbit gal bladder. *Amer. J. Physiol.* **205**:427.

Wright, E. M., Barry, P. H., Diamond, J. M. 1971. The mechanism of cation permea tion in rabbit gallbladder: Conductances, the current-voltage relation, the con centration dependence of anion-cation discrimination, and the calcium competitior effect. *J. Membrane Biol.* **4**:331.

— Diamond, J. M. 1968. Effects of pH and polyvalent cations on the selective perme ability of gall-bladder epithelium to monovalent ions. *Biochim. Biophys. Acta* **163**:57

— Prather, J. W. 1970. The permeability of the frog choroid plexus to nonelectrolytes *J. Membrane Biol.* **2**:127.